Eur. Phys. J. D **15**, 33–39 (2001)

**THE EUROPEAN PHYSICAL JOURNAL D**

EDP Sciences
© Società Italiana di Fisica
Springer-Verlag 2001

# Ionization of a hydrogen atom from its ground state by a coherent bichromatic laser field

M. Fifirig[1] and A. Cionga[2,a]

[1] Department of Chemistry, University of Bucharest, Bd. Regina Elisabeta 4-12, Bucharest 70346, Romania
[2] Institute of Space Sciences, P.O. Box MG-36, Bucharest-Magurele 76900, Romania

Received 31 August 2000 and Received in final form 6 February 2001

**Abstract.** We study the "coherent phase control" between the three-photon ionization by a fundamental laser field and the one-photon ionization by its third harmonic for a hydrogen atom in its ground state. The relative phase $\delta$ of the harmonic field with respect to the fundamental laser radiation "modulates" the interference between the two ionization channels, which is important near the crossing points between the ionization rates of the two individual processes. Numerical results for the total ionization rate and for the angular distribution of the photoelectrons as a function of the phase $\delta$ are presented for frequencies located in the vicinity of the atomic resonances corresponding to the absorption of two laser photons.

**PACS.** 32.80.Rm Multiphoton ionization and excitation to highly excited states (e.g., Rydberg states) – 32.80.Fb Photoionization of atoms and ions

## 1 Introduction

Multiphoton processes due to the simultaneous interaction with two or more fields of commensurate frequencies have been studied recently. The enhancement or decrement of the photoelectron spectra, of the high order harmonic generation yields, of the transition rates in molecules or semiconductors can be coherently controlled by varying both, the relative phase and the relative intensity of the harmonic field with respect to the fundamental [1].

A number of experimental [2–8] and theoretical [9–12] works investigated the interaction of an atom with a bichromatic electromagnetic field containing a fundamental frequency $\omega$ and its third harmonic $3\omega$. One of the reported results [8] refers to the modulation of the total ionization rate through quantum interference between a nonresonant three-photon ionization by the fundamental of a Nd:YAG laser and a single photon ionization by its third harmonic for sodium atoms initially prepared in the $3P_{1/2}$ excited state by the radiation of a dye laser. Other experiments [3] demonstrate the possibility of measuring the changes in the relative phase $\delta$ between the two commensurate laser fields. The experiment shows the interference between the single and three-photon processes corresponding to the $6s-6p$ transition induced in atomic mercury by a 185 nm and 554 nm laser beam. Reference [12] analyses a combination of phase and intensity control of integral and differential above-threshold ionization rates for first three ATI peaks. The first peak, associated with the two-photon paths involving the same $l$ states, is leading mainly to integral control. The other two peaks, reached by interfering quantum paths involving different $l$ states, are leading mainly to differential control. Figure 3 of this reference emphasizes the directional separation of one ATI peak from another, and the diversion of the alignment away from the light polarization direction.

There were experiments reported [13–15] in which the suppression of ionization through the $6s$ state of xenon by a destructive interference between the absorption of three fundamental photons of an IR laser and the reabsorption of the resonantly generated third harmonic was emphasized, when the laser was tuned in the vicinity of the three-photon resonance with the $6s$ state. The cancellation of four-photon resonances by interference between the absorption of three photons of the fundamental and one third harmonic photon was investigated by Elk, Lambropoulos and Tang [16].

The aim of this paper is to study the $1s$ state of a hydrogen atom interacting with an electromagnetic field consisting of the fundamental laser radiation and of its third harmonic. We investigate the ionization processes leading to photoelectrons of energy $E = E_1 + 3\hbar\omega$ ($E_1$ the ground state energy) in the particular case in which the absorption of two laser photons is not sufficient for ionization. We consider intensities for which the amplitude of the single-photon absorption yields a significant contribution to the amplitude of the ionization process.

[a] e-mail: aurelia_cionga@yahoo.com
or e-mail: cionga@venus.nipne.ro

In the vicinity of the two-photon resonances, the continuum state of energy $E$ can be reached by two main interfering paths:

(i) by three-photon absorption from the laser field;
(ii) by single-photon absorption of its harmonic.

We assume that the three-photon two-colour processes can be neglected close to these resonances.

In perturbation theory, using a nonrelativistic description, the calculations presented in Section 2 are done within the dipole approximation. The calculations are based on the analytic expression for the three-photon 1$s$-continuum matrix element derived previously [17] and already used in the study of the two-colour three-photon ionization of hydrogen [18]. Our numerical results for the total ionization rate and for the angular distribution of the photoelectrons are discussed in Section 3.

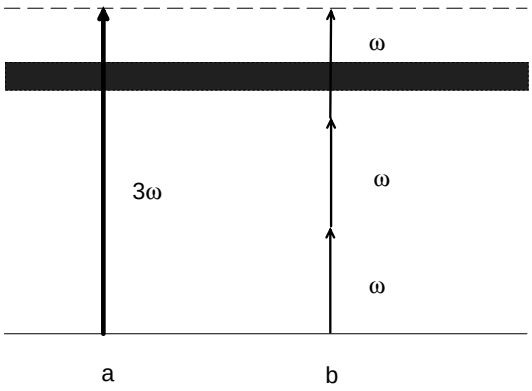


**Fig. 1.** Shows the leading diagrams associated with the process of ionization of the hydrogen atom, initially in its ground state, by the net absorption of the energy $3\hbar\omega$ in the bichromatic field composed of a laser source and its third harmonic.

## 2 Basic equations

We consider a hydrogen atom in its ground state interacting with an electromagnetic field described by the time-dependent vector potential

$$\mathbf{A}(t) = \frac{1}{2}\left[A_{0\mathrm{L}}\mathrm{e}^{\mathrm{i}\omega t} + A_{0\mathrm{H}}\mathrm{e}^{\mathrm{i}(3\omega t+\delta)}\right]\mathbf{s} + \text{c.c.}$$

We have denoted by $\omega$ the fundamental frequency of the laser. $A_{0\mathrm{L}}$ and $A_{0\mathrm{H}}$ are the amplitudes of the vector potentials of the laser and its harmonic, respectively, and $\delta$ stands for the relative phase of the third harmonic with respect to the fundamental. The two fields have identical polarizations $\mathbf{s}_{\mathrm{L}} = \mathbf{s}_{\mathrm{H}} = \mathbf{s}$, with the polarization vector $\mathbf{s}$ normalized such that $\mathbf{s}\cdot\mathbf{s}^* = 1$. We work in the velocity gauge, using the dipole approximation, and we treat the interaction with the bichromatic field as a perturbation.

In LOPT (lowest-order perturbation theory) for the transition from the ground state to the continuum of energy $E = E_1 + 3\hbar\omega$, we can associate one diagram of the first order in the fine structure constant $\alpha$ and ten diagrams of the third order in $\alpha$. One of these ten diagrams corresponds to the absorption of three identical photons of the laser, the other nine represent the radiative corrections to the absorption of one harmonic photon [19]. The amplitude of the above process of third order is proportional to

$$\left(\frac{eA_{0\mathrm{L}}}{2m_e}\right)^3\left[\mathcal{T}_{\mathrm{L}} + \frac{A_{0\mathrm{H}}}{A_{0\mathrm{L}}}\mathcal{T}_{\mathrm{C}} + \left(\frac{A_{0\mathrm{H}}}{A_{0\mathrm{L}}}\right)^3\mathcal{T}'_{\mathrm{C}}\right],$$

with $e$ the electron charge and $m_e$ its mass. The amplitude $\mathcal{T}_{\mathrm{L}}$ corresponds to the absorption of three photons of the laser, while $\mathcal{T}_{\mathrm{C}}$ and $\mathcal{T}'_{\mathrm{C}}$ refer to the radiative corrections due to the laser and the harmonic, respectively. We choose an intensity regime for which the rate of single-photon absorption has its largest value. In this regime, the ratio $A_{0\mathrm{H}}/A_{0\mathrm{L}}$ fulfils the condition

$$\frac{A_{0\mathrm{H}}}{A_{0\mathrm{L}}} = \frac{1}{3}\sqrt{\frac{I_{\mathrm{H}}}{I_{\mathrm{L}}}} < 10^{-2}.$$

Here we denoted the intensity of the laser and of the harmonic by $I_{\mathrm{L}}$ and $I_{\mathrm{H}}$, respectively. For the above intensity ratio, close to the two-photon resonance, we can neglect the correction terms. Hence, the continuum state of energy $E = E_1 + 3\hbar\omega$ can be reached by the two interfering paths presented in Figure 1:

(a) the single-photon absorption of the harmonic;
(b) the three-photon absorption from the fundamental laser field.

Correspondingly, the time-dependent perturbation theory for the ionization amplitude of the process shown in Figure 1 leads to

$$M = -2\pi\mathrm{i}\frac{eA_{0\mathrm{L}}}{2m_e}\left\{\frac{A_{0\mathrm{H}}}{A_{0\mathrm{L}}}\mathrm{e}^{-\mathrm{i}\delta}\mathcal{T}_{\mathrm{H}} + \left(\frac{eA_{0\mathrm{L}}}{2m_e}\right)^2\mathcal{T}_{\mathrm{L}}\right\}. \quad (1)$$

In the present paper, the subscripts "L" and "H" will always refer to the laser field and its harmonic, respectively. The amplitude $\mathcal{T}_{\mathrm{H}}$ of the single-photon absorption (the first diagram (a) of Fig. 1) is given by the expression

$$\mathcal{T}_{\mathrm{H}} = \mathcal{F}\,(\mathbf{n}\cdot\mathbf{s})\,,$$
$$\mathcal{F} = \frac{2\sqrt{2}}{\pi}\eta^{5/2}\mathrm{e}^{\pi\eta/2}\frac{\Gamma(2-\mathrm{i}\eta)}{(1+\eta^2)^2}\left(\frac{\mathrm{i}\eta-1}{\mathrm{i}\eta+1}\right)^{\mathrm{i}\eta}, \quad (2)$$

where $\mathbf{n} = \mathbf{p}/p$ denotes the direction of the photoelectron momentum $\mathbf{p}$ and $\eta = (\alpha m_e c)/p$ with $c$ being the velocity of the light.

The other amplitude $\mathcal{T}_{\mathrm{L}}$ corresponds to the diagram (b). It is constructed from the third-order tensor with Cartesian components

$$\Pi_{ijk}(\Omega',\Omega) = \langle E-|P_i G_{\mathrm{c}}(\Omega')P_j G_{\mathrm{c}}(\Omega)P_k|E_1\rangle, \quad (3)$$

where $\mathbf{P}$ is the momentum operator, $G_{\mathrm{c}}$ the Coulomb resolvent operator and $|E-\rangle$ and $|E_1\rangle$ are the final continuum (incoming) and initial ground state energy eigenvectors of the electron, respectively. The eigenvector $|E-\rangle$

is normalized in the energy and solid angle scales. The parameters $\Omega$ and $\Omega'$, relevant for our case, are

$$\Omega = E_1 + \hbar\omega, \qquad \Omega' = E_1 + 2\hbar\omega. \tag{4}$$

As was shown in references [17,18], the third-order tensor (3) can be expressed in terms of three invariant amplitudes $A$, $B$ and $C$ by

$$\Pi_{ijk} = \Upsilon[An_i\delta_{jk} + B(n_j\delta_{ki} + n_k\delta_{ij}) + Cn_in_jn_k]. \tag{5}$$

The quantity $\Upsilon$ is explicitly given by $\Upsilon = \sqrt{m_e}(\alpha c)^{-2}$. The amplitudes $A$, $B$ and $C$ are scalars, depending on $\Omega$, $\Omega'$ and $E$ only, and for our choice of normalization of $|E-\rangle$ they are dimensionless. They were derived previously [17,18] as a sequence of terms which are products of a hypergeometric Gauss function ${}_2F_1$ and a sum of several Appell functions $F_1$ [20]. Finally, the amplitude $\mathcal{T}_\mathrm{L}$ is given by

$$\mathcal{T}_\mathrm{L} = \mathbf{n}\cdot\mathbf{s}\left[(A+2B)\,(\mathbf{s})^2 + C\,(\mathbf{n}\cdot\mathbf{s})^2\right]. \tag{6}$$

In the absence of the harmonic field, the continuum state of energy $E = E_1 + 3\hbar\omega$ is reached through three photons absorption. The differential rate of the three-photon ionization of the ground state hydrogen is given by the expression

$$\frac{\mathrm{d}\Gamma_\mathrm{L}}{\mathrm{d}\Omega} = K\frac{1}{k^6}\left(\frac{I_\mathrm{L}}{I_0}\right)^3|\mathcal{T}_\mathrm{L}|^2, \tag{7}$$

where $K = (2\pi\alpha c)/a_0$, with $a_0$ denoting the Bohr radius, and $k \equiv \hbar\omega/|E_1|$ is the energy of the laser photon measured in Rydberg, where $I_0$ denotes the atomic unit for the radiation intensity. After integration over the directions of the ejected electron, the total rate for three-photon ionization reads

$$\Gamma_\mathrm{L} = \frac{4\pi K}{3k^6}\left(\frac{I_\mathrm{L}}{I_0}\right)^3\left(|S|^2 + \frac{12}{175}|C|^2\right), \tag{8}$$

with

$$S = A + 2B + \frac{3}{5}C. \tag{9}$$

On the other hand, if only the harmonic field is present, the differential rate $\mathrm{d}\Gamma_\mathrm{H}/\mathrm{d}\Omega$ and the total rate $\Gamma_\mathrm{H}$ of the corresponding photoelectric effect are given by

$$\frac{\mathrm{d}\Gamma_\mathrm{H}}{\mathrm{d}\Omega} = \frac{K}{9}\frac{1}{k^2}\frac{I_\mathrm{H}}{I_0}|\mathcal{T}_\mathrm{H}|^2, \tag{10}$$

$$\Gamma_\mathrm{H} = \frac{4\pi K}{27}\frac{1}{k^2}\frac{I_\mathrm{H}}{I_0}|\mathcal{F}|^2. \tag{11}$$

Finally, for the coherent superposition of the laser field and its third harmonic, the differential rate of ionization to the continuum state of energy $E = E_1 + 3\hbar\omega$ is given by the expression

$$\frac{\mathrm{d}\Gamma}{\mathrm{d}\Omega} = \frac{\mathrm{d}\Gamma_\mathrm{H}}{\mathrm{d}\Omega} + \frac{\mathrm{d}\Gamma_L}{\mathrm{d}\Omega} + 2\sqrt{\frac{\mathrm{d}\Gamma_\mathrm{H}}{\mathrm{d}\Omega}\frac{\mathrm{d}\Gamma_\mathrm{L}}{\mathrm{d}\Omega}}\cos\left[\delta + \arg\mathcal{T}_\mathrm{L} - \arg\mathcal{T}_\mathrm{H}\right], \tag{12}$$

where $\exp(\mathrm{i}\arg\mathcal{T}_\mathrm{L}) = \mathcal{T}_\mathrm{L}/|\mathcal{T}_\mathrm{L}|$ and similarly for $\arg\mathcal{T}_\mathrm{H}$. The last term in equation (12) is the relevant interference term. According to (2, 6, 7, 10), the above differential rate gets modulated by the over-all factor $|\mathbf{n}\cdot\mathbf{s}|^2$.

The interference effects are much better illustrated by the total rate, found to be

$$\Gamma = \Gamma_\mathrm{L} + \Gamma_\mathrm{H} + \frac{6}{k^2}\frac{I_\mathrm{L}}{I_0}\sqrt{\frac{\Gamma_\mathrm{L}}{\Gamma_\mathrm{H}}}\Gamma_\mathrm{H}\left|\frac{S}{\mathcal{F}}\right|\cos\left(\delta + \arg S - \arg\mathcal{F}\right), \tag{13}$$

where the interference and geometrical effects do not get mixed. The last term in the equation (13) is again the interference term. The total rate has a maximum for a phase difference $\delta = \arg\mathcal{F} - \arg S$, and a minimum for $\delta = \pi + \arg\mathcal{F} - \arg S$. We expect significant interference effects for those laser frequencies for which the two independent rates $\Gamma_\mathrm{L}$ (8) and $\Gamma_\mathrm{H}$ (11) are approximately equal.

## 3 Numerical results

We present results for the ionization of the hydrogen ground state by a bichromatic field of frequencies $\omega$ and $3\omega$ leading to photoelectrons of the energy of $E = E_1 + 3\hbar\omega$. The two components of the field are weak and have identical linear polarizations. The cases discussed here refer to the situation in which the absorption of two laser photons is not sufficient for ionization: $2\hbar\omega < |E_1| < 3\hbar\omega$. In general, if the intensities of the two components satisfy the condition

$$\gamma = \frac{I_\mathrm{L}}{I_\mathrm{H}}\left(\frac{I_\mathrm{L}}{I_0}\right)^2 < 10^{-4}, \tag{14}$$

the rate for single photon absorption is larger than the one for three-photon absorption, except for those frequency domains which are the closest to the resonances of the latter process. In the vicinity of two-photon resonances, where $2\hbar\omega \simeq E_n - E_1$ with $n \geq 2$, the continuum state can be reached by the two competing paths shown in Figure 1. The other contributions, due to two-colour three-photon processes, are negligible. In this frequency domain we evaluated the Appell hypergeometric functions entering the amplitudes $A$, $B$ and $C$ through their series expansions as in reference [18].

The first set of results (Figs. 2a–2c) show the three-photon ionization rate $\Gamma_\mathrm{L}$ (dotted curve) and the single-photon ionization rate $\Gamma_\mathrm{H}$ (chain curve) as a function of the laser wavelength $\lambda$ in the region between 190 and 260 nm. Both curves are scaled by the harmonic intensity $I_\mathrm{H}$. We have chosen three pairs of intensities such that $\gamma = 10^{-4}, 10^{-5}, 10^{-6}$. More precisely, we have $I_\mathrm{L}/I_\mathrm{H} = 10^4$, $I_\mathrm{L}/I_0 = 10^{-4}$ in Figures 2a and 2d, $I_\mathrm{L}/I_\mathrm{H} = 10^3$, $I_\mathrm{L}/I_0 = 10^{-4}$ in Figures 2b and 2e and $I_\mathrm{L}/I_\mathrm{H} = 10^4$, $I_\mathrm{L}/I_0 = 10^{-5}$ in Figures 2c and 2f. In the panels (a), (b) and (c), the curves showing three-photon ionization rates present three peaks related to atomic resonances given by two-photon virtual excitation of the intermediate state.

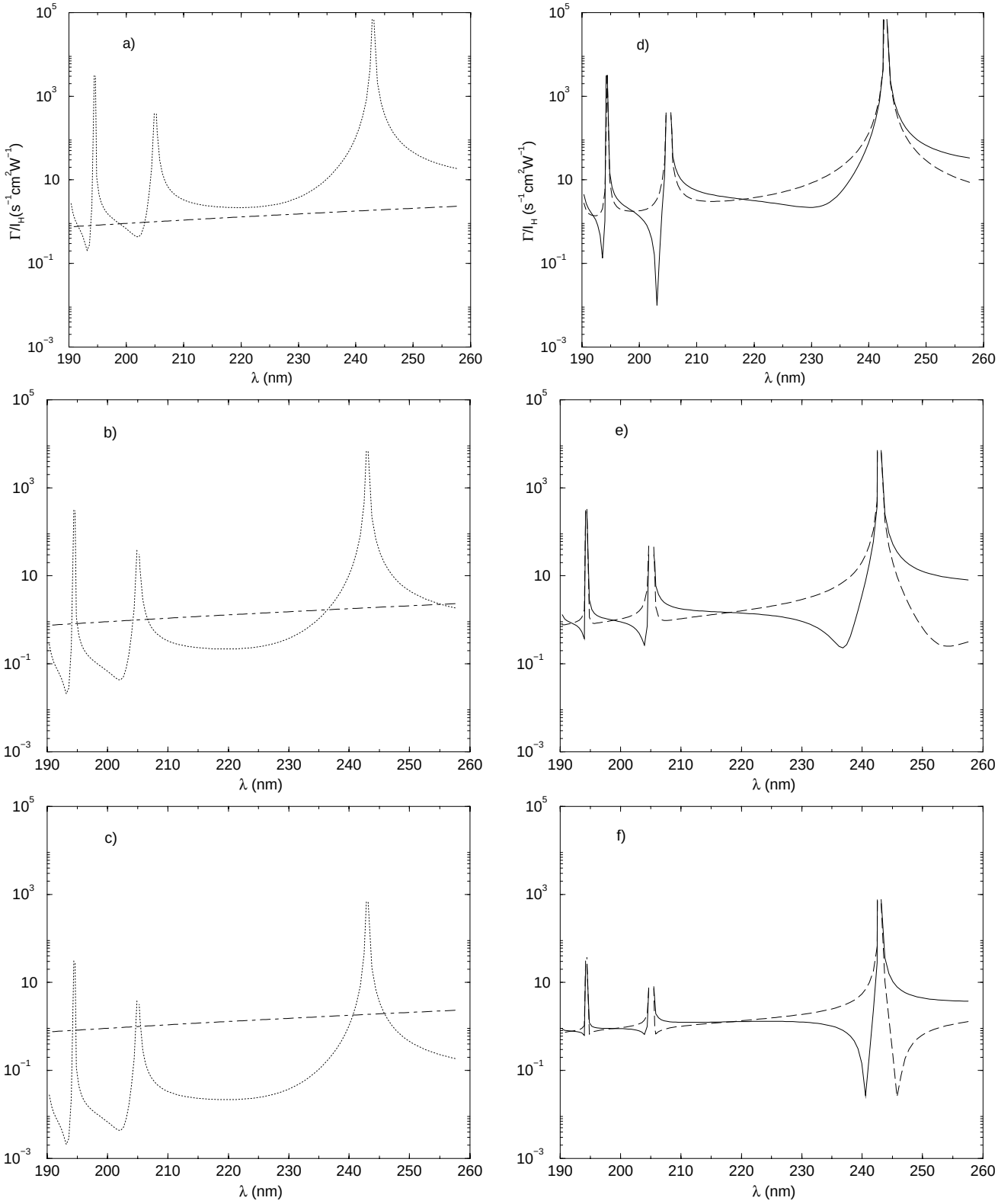


**Fig. 2.** (a) Presents the total three-photon ionization rate $\Gamma_{\rm L}/I_{\rm H}$ (dotted curve) and single-photon ionization rate $\Gamma_{\rm H}/I_{\rm H}$ (chain curve), each divided by the intensity of the harmonic field, as function of the laser wavelength $\lambda$ for identical linear polarizations and $I_{\rm L}/I_{\rm H} = 10^4$, $I_{\rm L}/I_0 = 10^{-4}$. (b) The same as in (a) for $I_{\rm L}/I_{\rm H} = 10^3$, $I_{\rm L}/I_0 = 10^{-4}$. (c) Like in (a) for $I_{\rm L}/I_{\rm H} = 10^4$, $I_{\rm L}/I_0 = 10^{-5}$. (d) The total photoionization rate (13) in the bichromatic field as function of the laser wavelength $\lambda$ for two values of the phase difference $\delta = 0^\circ$ (full curve) and $\delta = 180^\circ$ (broken curve) and intensity ratios: $I_{\rm L}/I_{\rm H} = 10^4$, $I_{\rm L}/I_0 = 10^{-4}$. (e) The same as in (d) for equal intensities as in (b). (f) The same as in (d) for equal intensities as in (c).

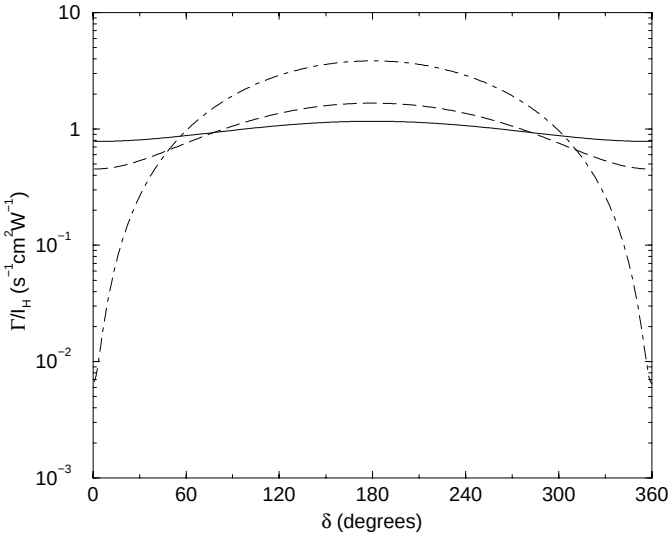


**Fig. 3.** Shows the phase-dependence of the two-colour ionization rate $\Gamma/I_{\rm H}$ for $I_{\rm L}/I_0 = 10^{-4}$, laser wavelength $\lambda =$ 203.2 nm and several values of the intensity ratios $I_{\rm L}/I_{\rm H} =: 10^2$ (full curve), $10^3$ (broken curve) and $10^4$ (chain curve).

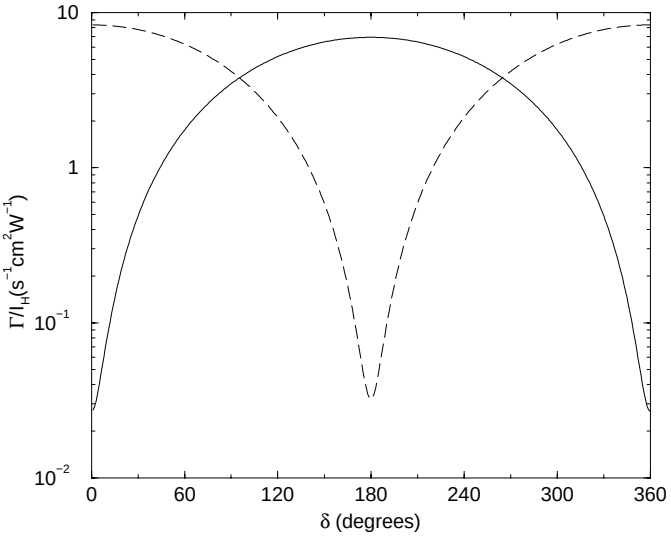


**Fig. 4.** Demonstrates the influence of the laser wavelength on the phase-dependence of the two-colour ionization rate for $I_{\rm L}/I_{\rm H} = 10^4$, $I_{\rm L}/I_0 = 10^{-5}$ and two values of $\lambda =: 240.6$ nm (full curve), 245.6 nm (broken curve).

The resonance at $\lambda = 243.1$ nm is due to the intermediate state $2s$, while each of the other two resonances, $\lambda = 205.3$ nm and $\lambda = 194.5$ nm are due to two intermediate states $ns$, $nd$ with $n = 3$ and $n = 4$, respectively. The plotted quantities are multiplied by a factor $10^{15}$. The parameter $\gamma$ has decreasing values: it is $10^{-4}$ in panel (a), $10^{-5}$ in panel (b) and $10^{-6}$ in panel (c), leading to a downward shift of the dotted curve for three photon ionization. Strong interference effects are expected for that laser wavelength which corresponds to the crossing points between three-photon ionization rate, $\Gamma_{\rm L}$, and single-photon ionization rate $\Gamma_{\rm H}$. The other three (Figs. 2d–2f) show the wavelength dependence of the photoionization rate (13) for two values of the relative phase: $\delta = 0°$ (full curve) and $\delta = 180°$ (broken curve). In panel (d) the interference effect is rather small for $\lambda = 243.1$ nm. Indeed, close to this resonance there are no crossing points between the two curves in panel (a) for $\gamma = 10^{-4}$. On the contrary, for the same wavelength, striking interference effects are present in panel (f). The crossing points related to the other two resonances are too close to each other in panel (c), leading to minor interferences.

Figure 3 illustrates the phase-dependence of the two-colour total ionization rate (13) normalized with respect to $I_{\rm H}$, for the laser wavelength $\lambda = 203.2$ nm. For the intensities chosen in Figures 2a and 2b this wavelength is close to the crossing point near the resonance $\lambda =$ 205.3 nm. One can see that for a given value of the laser intensity the interference effects also depend on the relative intensity $I_{\rm H}/I_{\rm L}$. The data plotted in Figure 3 belong to the same laser field $I_{\rm L} = 10^{-4} I_0$ but to three different values of the relative intensity, namely $I_{\rm L}/I_{\rm H} = 10^2$ (full curve), $I_{\rm L}/I_{\rm H} = 10^3$ (broken curve) and $I_{\rm L}/I_{\rm H} = 10^4$ (chain curve). We mention that the last two curves refer to the intensities used in panels 2b and 2a, respectively. The strongest interference effects (where the ratio between the maximum and the minimum of $\Gamma/I_{\rm H}$ is the largest) are obtained for $I_{\rm L}/I_{\rm H} = 10^4$ in agreement with a direct comparison between Figures 2d and 2e.

The influence of the laser wavelength on the phase-dependence of the ionization rate (13) is shown in Figure 4. In this figure we chose $I_{\rm L}/I_{\rm H} = 10^4$, $I_{\rm L}/I_0 = 10^{-5}$ ($\gamma = 10^{-6}$) and two values of $\lambda$: 240.6 nm (full curve), 245.6 nm (broken curve). This situation corresponds to the graphs 2c and 2f. The first wavelength is close to the crossing point situated before the resonance at 243.1 nm and the latter is near the crossing point located after the resonance. At $\delta = 180°$ the interference effects are constructive for $\lambda = 240.6$ nm, while for $\lambda = 245.6$ nm they are destructive.

In Figure 5 we present the angular distribution given by equation (12) as polar diagrams, for $I_{\rm L}/I_{\rm H} = 10^4$, $I_{\rm L}/I_0 = 10^{-4}$, $\lambda = 194$ nm and three values of the phase difference $\delta$: 0° (full curve), 90° (broken curve) and 180° (chain curve). The wavelength chosen is located in the vicinity of the crossing point situated before the resonance 194.5 nm (see panel 2a). The polarization vectors are linear, identical and determine the $z$-axis. In this case $\mathbf{n} \cdot \mathbf{s} = \cos\theta$, where $\theta$ is the angle between the direction of the ejected electron and the $z$-axis. In our Figure 5, the polarization axis is depicted by the horizontal line. The polar diagrams present two zeros at 90° and 270° because of the over-all $\cos^2\theta$ factor in the expression (12). Their magnitude and shape are strongly influenced by the phase difference $\delta$. As expected, for $\delta = 180°$, the magnitude of the lobes is largest. It should be noted that for the value of the intensity parameter chosen in this figure ($\gamma = 10^{-4}$), the lobes and implicitly the differential ionization rate are aligned about the polarization direction represented here by horizontal line.

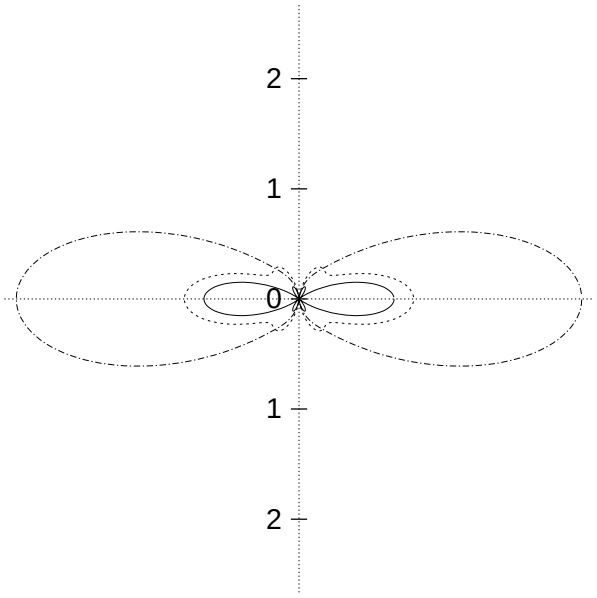


**Fig. 5.** Presents the angular distribution of the differential rates (12) as polar diagrams, for $I_{\rm L}/I_{\rm H} = 10^4$, $I_{\rm L}/I_0 = 10^{-4}$, $\lambda = 194$ nm and three values of the phase difference $\delta =:$ $0^\circ$ (full curve), $90^\circ$ (broken curve) and $180^\circ$ (chain curve). The polar angle $\theta$ is measured from the horizontal line that represents the polarization axis.

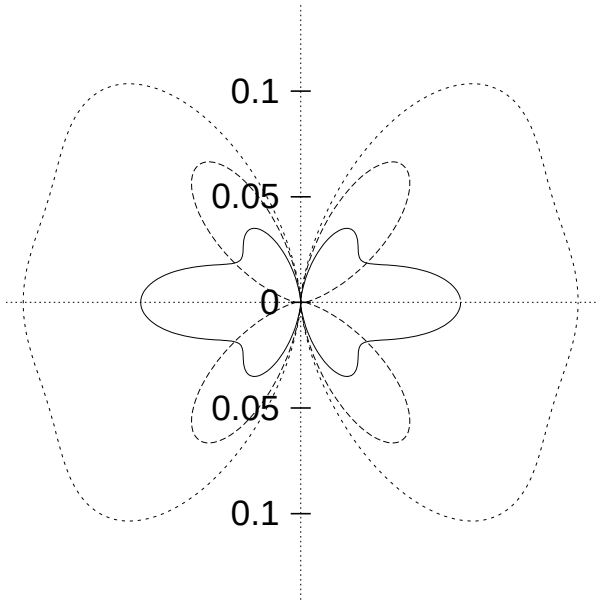


**Fig. 6.** Same as Figure 5 but for $I_{\rm L}/I_{\rm H} = 10^3$, $I_{\rm L}/I_0 = 10^{-4}$. The three values of the phase difference $\delta$ are $0^\circ$ (full curve), $40^\circ$ (long-broken curve) and $90^\circ$ (short-broken curve).

In order to check the ability of this perturbative approach to predict intensity and phase control of alignment away from the polarization direction we evaluate the differential ionization rate for $\gamma = 10^{-5}$ and the same laser wavelength as in Figure 5. The data are plotted in Figure 6 for $\delta = 0^\circ$ (full curve), $\delta = 40^\circ$ (long-broken curve) and $\delta = 90^\circ$ (short-broken curve). The differential rates have a fourfold symmetry: the polarization and propagation directions of the laser represent symmetry axes of our polar graphs. At $\delta = 0^\circ$ we observe four side lobes whose magnitude grows with the increasing of $\delta$. Simultaneously, the magnitude of the lobes aligned along the polarization vector decreases. At $\delta = 40^\circ$ the side lobes are the only prominent ones, those aligned along the polarization vector are extinct. The side lobes are aligned along the $\theta = 53^\circ$ and $\theta = 127^\circ$, respectively. The contribution of the "side lobes" remains important even at $\delta = 90^\circ$ leading to broad angular distribution. A comparison between our Figures 5 and 6 reveals that a particular combination of the field intensities and phase difference changes the alignment of the differential ionization rate. A similar effect was shown previously in Figure 3 of the reference [12] for a different set of parameters.

## 4 Summary

We have investigated the ionization of a hydrogen atom from its ground state interacting simultaneously with a laser field and its third harmonic. The transition to a continuum state of energy corresponding to the net absorption of the energy $3\hbar\omega$ is discussed only. Using time-dependent perturbation theory, the calculation is performed in the dipole approximation and in the velocity gauge. We were interested in the present investigation in those intensity regimes for which the amplitude of the single-photon absorption has a significant contribution as compared with the three-photon absorption process. The interference effects are expected to dominate near the two-photon resonances. In this case the continuum state can be reached by two main paths:

(i) the three-photon absorption from the fundamental laser field;
(ii) the single-photon absorption from the harmonic field.

The numerical results illustrate the strong dependence of the total ionization rate and of the angular distribution of the differential ionization rates on the phase difference $\delta$, on the relative intensity $I_{\rm L}/I_{\rm H}$ of the laser field and its harmonic and on the laser frequency $\omega$. For a particular combination of the fields intensities and of the harmonic phase with respect to the fundamental, the differential ionization rate can be diverted away from the polarization direction.

The numerical calculations were performed on the workstation HP-715 of the Computer Center of the Quantum and Statistical Physics Group (Bucharest-Magurele), a donation of the SOROS Foundation. The authors are grateful to V. Florescu for useful discussions, encouragements and criticism of this work.

## References


1. M. Shapiro, P. Brumer, Adv. At. Mol. Opt. Phys. **42**, 287 (2000).
2. Ce Chen, Yi-Yian Yin, D.S. Elliott, Phys. Rev. Lett. **64**, 507 (1990).
3. Ce Chen, D.S. Elliott, Phys. Rev. Lett. **65**, 1737 (1990).
4. S. Watanabe, K. Kondo, Y. Nabekawa, A. Sagisaka, Y. Kobayaski, Phys. Rev. Lett. **73**, 2692 (1994).
5. M.D. Perry, J.K. Crane, Phys. Rev. A **48**, R4051 (1993).
6. D.A. Telnov, J. Wang, Shih-I Chu, Phys. Rev. A **52**, 3988 (1995).
7. G.G. Paulus, W. Becker, H. Walther, Phys. Rev. A **52**, 4043 (1995).
8. S. Cavalieri, R. Eramo, L. Fini, Phys. Rev. A **55**, 2941 (1997).
9. R.M. Potvliege, P.H.G. Smith, J. Phys. B: At. Mol. Opt. Phys. **24**, L641 (1991); **25**, 2501 (1992).
10. A. Szoke, K.C. Kulander, J.N. Bardsley, J. Phys. B: At. Mol. Opt. Phys. **24**, 3165 (1991).
11. M. Protopapas, P.L. Knight, K. Burnett, Phys. Rev. A **49**, 1945 (1994).
12. R.A. Blank, M. Shapiro, Phys. Rev. A **52**, 4278 (1995).
13. J.C. Miller, R.N. Compton, M.G. Payne, W.R. Garrett, Phys. Rev. Lett. **45**, 114 (1980).
14. D.J. Jackson, J.J. Wynne, P.H. Kes, Phys. Rev. A **28**, 781 (1983).
15. P.R. Blazewicz, J.C. Miller, Phys. Rev. A **38**, 2863 (1988).
16. M. Elk, P. Lambropoulos, X. Tang, Phys. Rev. A **44**, R31 (1991).
17. A. Cionga, M. Vatasescu, M. Fifirig, V. Florescu, Rom. Rep. Phys. **46**, 441 (1994).
18. M. Fifirig, A. Cionga, V. Florescu, J. Phys. B: At. Mol. Opt. Phys. **30**, 2599 (1997).
19. R. Shakeshaft, J. Opt. Soc. Am. B **5**, 705 (1987); see also M. Edwards, R. Shakeshaft, Z Phys. D **8**, 51 (1988).
20. P. Appell, J. Kampé de Fériet, *Fonctions Hypergéométriques et Hypersphériques. Polynômes d'Hermite* (Gauthier-Villars, Paris, 1926), Ch. I.